

MODELING AND EXPERIMENTAL STUDIES OF BEAM HALO AT ATF2*

R. Yang[†], P. Bambade, V. Kubytskyi, Laboratoire de l'Accélérateur Linéaire (LAL), Universite Paris-Sud, CNRS/IN2P3, Orsay, France

A. Faus-Golfe, N. Fuster-Martínez, Instituto de Física Corpuscular(IFIC), Valencia, Spain
T. Naito, High Energy Accelerator Research Organization (KEK), Tsukuba, Japan

Abstract

The Accelerator Test Facility 2 (ATF2) at KEK is a prototype of the final focus system for the next generation of Future Linear Colliders(FCL). It aims to focus the beams to tens of nanometer transverse sizes and to provide stability at the few nm level. Achieving these goals requires modelling, measuring and suppressing of the transverse beam halo before the interaction point (IP). This paper presents a beam tail/halo generator based on realistic model and the investigation of vertical and horizontal beam tail/halo distribution at ATF2.

INTRODUCTION

As a proof-of-principle facility for FLC, ATF2 aims to demonstrate the 37 nm beam size at Interaction Point (IP) and its stability at nanometers level [1]. Beam loss due to beam halo hitting the beam pipe is the main source of background affecting the measurement of the nm scale beam sizes using a laser interferometer beam size monitor (Shintake monitor [2]).

In order to investigate the formation and behaviour of beam tail/halo, theoretical analysis, simulation and measurement have been performed. Theoretical calculation suggests that the elastic beam gas scattering, which is dependent on the damping ring (DR) vacuum, should be the main source of beam halo at ATF [3,4]. To estimate the beam halo behaviour along ATF2, particle tracking and realistic modelling based on the measurement are used. These studies require an independent 4 dimensions distribution (x, x', y, y') based on a realistic model. To study beam tail/halo sources at ATF2, several devices are developed including the Wire Scanner (WS), YAG:Ce screen and OTRs [5,6]. They can measure the beam core and beam tail/halo quickly but with a limited dynamic range. With great sensitivity (sensitive to single electrons) and high dynamic range ($\sim 10^6$), an in vacuum Diamond Sensor (DS) has been developed and installed [7]. Recently, the vertical beam halo has been measured using YAG screen and DS at ATF2 [5,7]. However, no systematic studies are performed to investigate the formation of both vertical and horizontal beam tail/halo at ATF. In this paper, a beam halo generator based on realistic model is introduced at first. Then, the experimental investigations of beam halo distribution and formation in the vertical and horizontal plane are presented.

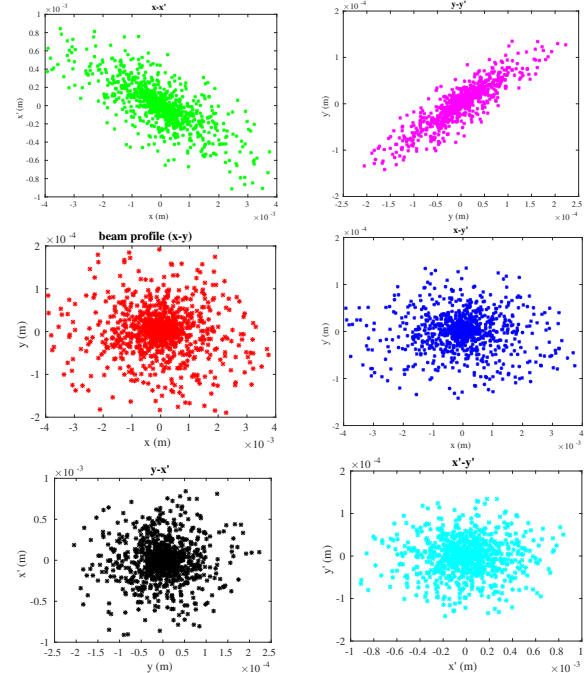


Figure 1: Transverse phase-space distributions with realistic model.

REALISTIC BEAM HALO GENERATOR

In 2005, the first measurement of beam halo at the EXT line of ATF was performed using a WS [2]. Assuming a Gaussian distribution for the beam core ($< 3\sigma$), the beam tail/halo distribution could be parameterized as

$$\rho_H = 2.2 \times 10^9 X^{-3.5} \quad (1)$$

$$\rho_V = \begin{cases} 2.2 \times 10^9 X^{-3.5} & 3 < X < 6 \\ 3.7 \times 10^8 X^{-2.5} & X > 6 \end{cases} \quad (2)$$

where ρ_H and ρ_V are the horizontal and vertical distributions, $X = x/\sigma_x$ is the number of sigmas. We define the normalized variables $\tilde{x} = \frac{x}{\sqrt{\beta}}$ and $\tilde{x}' = \frac{dx}{d\phi} = \sqrt{\beta}x' + x\frac{\alpha}{\sqrt{\beta}}$. The Courant-Snyder invariant can be expressed as

$$\tilde{x}^2 + \tilde{x}'^2 = \gamma x^2 + 2\alpha x x' + \beta x'^2 = \frac{\varepsilon}{\pi} \quad (3)$$

The \tilde{x} and \tilde{x}' are independent and with the same distribution function. For simplicity, we assume the vertical tail/halo distribution to be same as the horizontal one, see Eq.(1). Due to circular symmetry, the distributions of $(\tilde{x}, \tilde{x}', \tilde{y}, \tilde{y}')$ will be independent and share the same shape. The 4D distribution

* Work supported by Chinese Scholarship Council

[†] ryang@lal.in2p3.fr

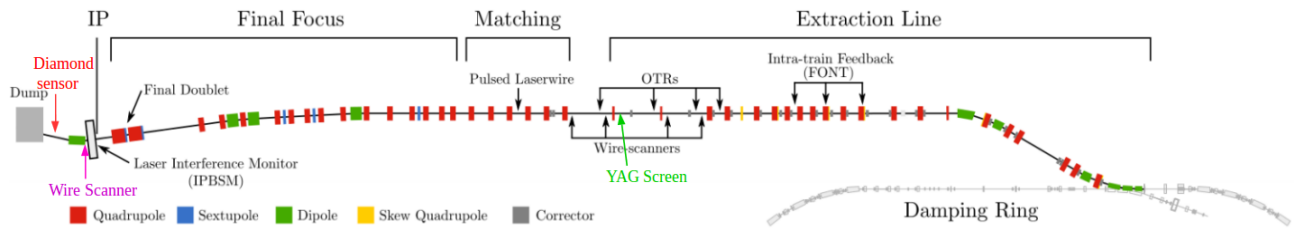


Figure 2: Schematic of ATF2 beam line with diagnostic devices.

can be described as

$$f(r) = \begin{cases} \frac{N}{\sqrt{2\pi}\sigma_r} e^{-\frac{r^2}{2\sigma_r^2}} & |r| \leq 3\sigma_r \\ NK_1 \cdot r^{-3.5} & 3\sigma_r < |r| < 40\sigma_r \end{cases} \quad (4)$$

where $r = \sqrt{\tilde{X}^2 + \tilde{X}'^2 + \tilde{Y}^2 + \tilde{Y}'^2}$, N is the quantity of particles and K_1 is a matching factor.

The generating procedure is the following: firstly, decide the number of particles in beam core and beam halo regions according to the measurement; secondly, generate the beam core and beam halo particles r_j respectively, as normalized coordinates using a Monte Carlo algorithm; thirdly, assign each r to $(\tilde{X}, \tilde{X}', \tilde{Y}, \tilde{Y}')$ randomly; and last, convert the normalized distributions $(\tilde{X}, \tilde{X}', \tilde{Y}, \tilde{Y}')$ to the physical phase space distribution (x, x', y, y') . The beam distributions generated with the above method are independent and without any coupling between (x, x') and (y, y') planes, as shown in Fig. 1.

BEAM HALO MEASUREMENT

The ATF2 beam line consists of three sections: the Extraction Line (EXT), the Final Focus System (FFS) and the Post-IP line. The location of the devices used to study the beam halo are shown in Fig. 2. An vertical YAG:Ce screen is installed in EXT line as described in Ref. [5]. In the Post-IP line, there are 2 wire scanners and 2 DS detectors installed recently. During the experiments period, BX10BY1 optics (the nominal β_y and 10 times the nominal β_x) was used with $0.1 \times 10^{10}/\text{pulse}$ beam intensity.

Vertical Beam Halo Measurement at ATF2

A YAG:Ce screen, which has a 1 mm slit in the center to allow the beam core to go through with little interaction, has been developed to visualize the beam halo distribution at the EXT line. Only the beam halo hits the screen and the fluorescent light is observed by a CCD camera. Higher beam tail /halo level was observed clearly when the DR vacuum increased from 5.2×10^{-7} Pa, 9.6×10^{-7} Pa to 15.5×10^{-7} Pa with low beam intensity, as shown in Fig. 3. The beam tail/halo measured has the same magnitude as the theoretical expectation based on beam-gas elastic scattering [5, 8]. Especially for the 9.7×10^{-7} Pa case, the shape and distribution agree well with theoretical predictions.

In the Post-IP, a WS with more than 10^4 dynamic range is located downstream of the IP. The vertical beam profile

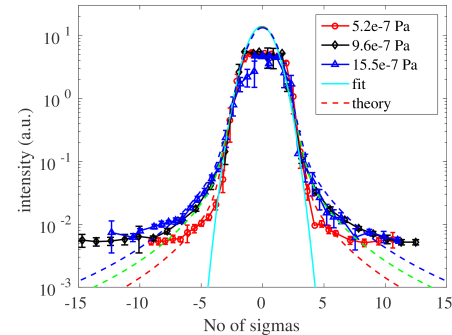


Figure 3: Beam halo distribution at EXT line.

agrees well with the tracking results, as shown in Fig. 4. The tracking is performed using MAD-X based on an initial distribution described in Eq.(4) with the full optics of ATF2, including higher order multipoles. It indicates that the distribution of vertical beam tail/halo at the Post-IP location is mainly determined by the extracted beam from the DR. There is no significant enhancement of beam tail/halo along ATF2.

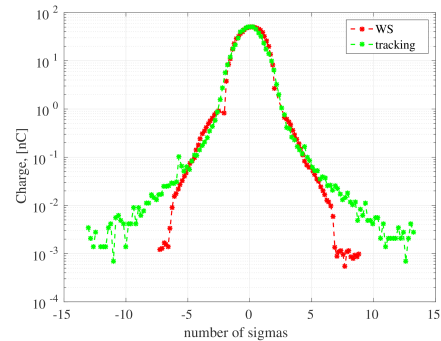


Figure 4: Beam profile imaged by WS at Post-IP (the edges on the two sides are cuts by a vertical collimator).

With the *in vacuum* diamond sensor, which has a high dynamic range ($\sim 10^6$), we investigated the vertical beam profiles in the Post-IP line with different DR vacuum levels. The beam tail/halo is higher than the tracking result, however it does follow the DR vacuum, as shown in Fig. 5. The reason could be the imperfect horizontal alignment of the beam with respect to the center of DS during the vertical scanning. It will induce some enhancement of the beam tail/halo distribution, see Fig. 5. The edges on the left and right sides are cuts by the aperture of the bending magnet before the DS.

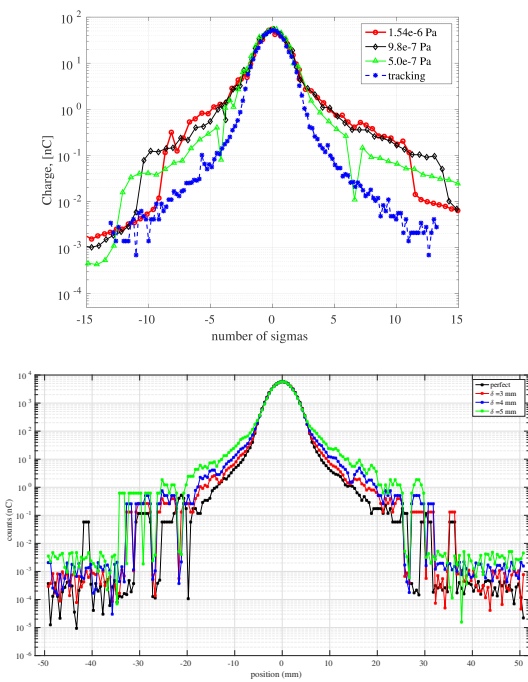


Figure 5: Upper: vertical beam profile measured by DS; Lower: vertical beam profile with horizontal misalignments.

In addition, the beam profile with different beam intensities is also measured using DS, as shown in Fig. 6. Beam size increases corresponding to beam intensity due to intra-beam scattering [9]. However, beam tail/halo are consistent for different beam intensities after normalizing to the same intensity.

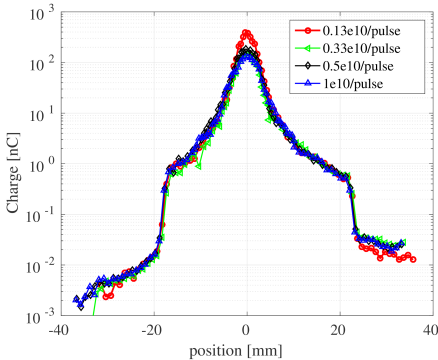


Figure 6: Vertical beam profile with different beam intensities.

Horizontal Beam Profile Measurement at Post-IP

The horizontal beam profile is only measured using the DS for various DR vacuum levels, as shown in Fig. 7. The beam profile can be normalized to the number of sigmas and fit to

$$f(X) = \begin{cases} \frac{N}{\sqrt{2\pi}} e^{-\frac{X^2}{2}} & 0 < X < 4 \\ NK_x X^{-4.5(-4.2)} & X > 4 \end{cases} \quad (5)$$

where $X = x/\sigma_x$, N is the total charge signal, K_x is the matching factor. The boundary of beam core and tail/halo is

$4\sigma_x$ which is defined by comparing the beam profile with the Gaussian beam core distribution. The beam tails/halo on the left and right sides are fit with different exponents -4.5 and -4.2 because of an asymmetric distribution. A good agreement of beam tail /halo in magnitude is observed between the measurement and tracking result. But the beam tail/halo didn't increase obviously as a function of the vacuum level in the DR, which indicates that the main source of horizontal beam halo at ATF2 might not be the beam-gas scattering.

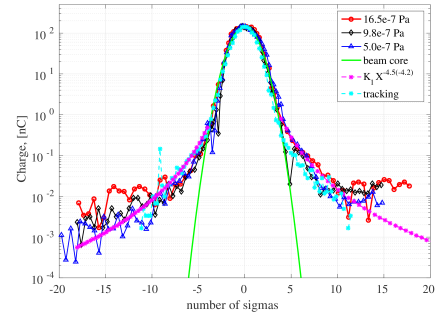


Figure 7: Horizontal beam profile at Post-IP.

CONCLUSION AND PROSPECTS

A realistic beam halo generator was developed to get the 4D distribution. Following this method, we can generate an independent distribution without coupling between (x, x') and (y, y') plane.

In ATF2, the beam tail/halo distribution is being investigated with several devices. Vertically, the beam halo distributions measured in the EXT line using a YAG:Ce screen and at the Post-IP using a DS are functions of the DR vacuum level. From the comparison of the measurements with the theoretical predictions we can conclude that the vertical beam tail/halo distribution is mainly due to the elastic beam gas scattering in the DR. In the case of the measurements done with the DS, the beam tail/halo is higher than expected. One possible reason could be an imperfect horizontal alignment of the beam with respect to the center of the DS. Horizontally, the beam halo is only probed by the DS at the Post-IP. The measurements correspond to the tracking results but the increase of beam tail/halo as a function of DR vacuum level isn't observed.

In the future, more detailed experimental studies of beam halo at ATF with different DR and beam conditions are proposed. Theoretical studies of beam halo formation in ATF DR are also suggested.

ACKNOWLEDGEMENT

We thank S. Bai, K. Kubo, X. Li, S. Liu, T. Tauchi, N. Terunuma, S. Wallon and D. Wang for helpful discussions, comments and commissioning assistances.

REFERENCES

- [1] Grishanov *et al.*, "ATF2 proposal", 2005.
- [2] S. Taikan *et al.*, "A nanometer beam size monitor for ATF2.", *Nucl. Inst. Meth.*, vol. 616D(1), pp. 1-8, 2010.

- [3] H. Kohji and K. Yokoya, "Non-Gaussian distribution of electron beams due to incoherent stochastic processes", KEK, 1992.
- [4] K.L.F. Bane *et al.*, "Intrabeam scattering analysis of measurements at KEK's Accelerator Test Facility damping ring", *Phys. Rev. ST Accel. Beams*, vol. 5, p.084403, 2002.
- [5] T. Naito and T. Mitsuhashi, in *Proc. IBIC'15*, pp. 373–376.
- [6] N. Fuster-Martinez *et al.*, in *Proc. IPAC'15*, pp. 3–10.
- [7] S. Liu *et al.*, "In vacuum diamond sensor scanner for beam halo measurements in the beam line at the KEK Accelerator Test Facility", submitted for publication.
- [8] T. Naito and T. Mitsuhashi, in *Proc. IBIC'14*, pp. 426–429.
- [9] K. Kubo *et al.*, "Extremely low vertical-emittance beam in the Accelerator Test Facility at KEK.", *Phys. Rev. Lett.*, vol. 88, no.19, p.194801, 2002